IEEE Photonics Journal
An IEEE Photonics Society Publication

Open Access

Optical Single Sideband Modulator Without Second-Order Sidebands

Volume 10, Number 3, June 2018

Erwin Hoi Wing Chan
Chongjia Huang
Chirappanath B. Albert

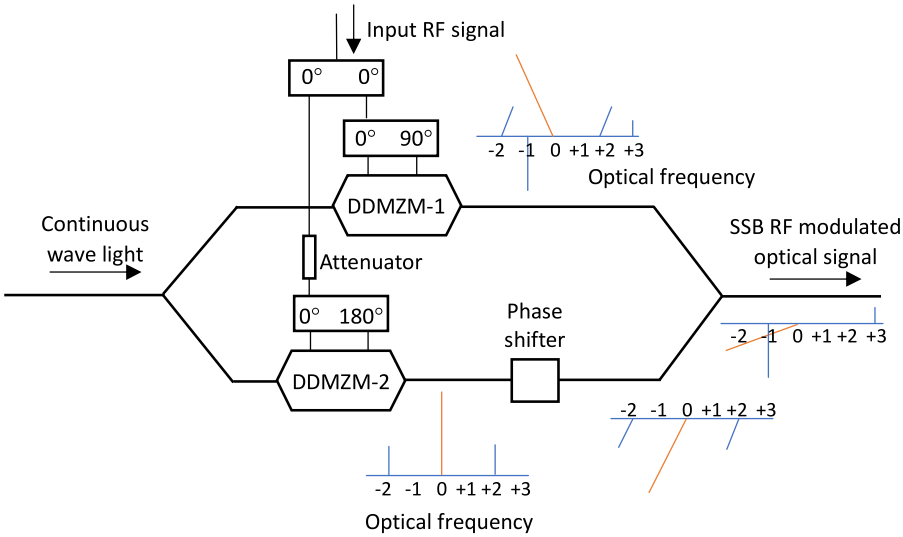

DOI: 10.1109/JPHOT.2018.2835810
1943-0655

Optical Single Sideband Modulator Without Second-Order Sidebands

Erwin Hoi Wing Chan, Chongjia Huang, and Chirappanath B. Albert

School of Engineering and Information Technology, Charles Darwin University, Darwin, NT 0909 Australia

DOI:10.1109/JPHOT.2018.2835810

Manuscript received April 3, 2018; revised May 6, 2018; accepted May 9, 2018. Date of publication May 21, 2018; date of current version June 1, 2018. Corresponding author: Erwin Hoi Wing Chan (e-mail: erwin.chan@cdu.edu.au).

Abstract: An optical single sideband modulator without generating both the −2nd- and +2nd-order sidebands is presented. It is based on a parallel operation of two dual-drive Mach–Zehnder modulators (DDMZMs) where one is operated as a conventional single sideband (SSB) modulator and the other is operated as a single-drive Mach–Zehnder modulator (MZM) biased at the maximum transmission point. The 2nd-order sidebands generated by the SSB modulator and the maximum-biased MZM can be cancelled by controlling the sideband amplitude and phase. Canceling the 2nd-order sidebands eliminates the second-order harmonic component presented at the output of a long-reach fiber optic link. The new SSB modulator can be implemented using standard off-the-shelf components and has a wide bandwidth. Experimental results show >20 dB 2nd-order sidebands suppression for different modulation indexes and 22.6 dB reduction in the fiber optic link output second-order harmonic component, compared to using a conventional SSB modulator formed by a DDMZM and a 90° hybrid coupler. Results also demonstrate that the performance of the new SSB modulator is insensitive to the optical carrier frequency and the input RF signal frequency.

Index Terms: Fiber optics links and subsystems, optical communications, radio frequency photonics, modulators.

1. Introduction

Fibre optic links (FOLs) contribute extensively to the field of long distance radio-over-fibre systems [1]. A wide range of applications such as military warfare, radio astronomy, cable television distribution networks and sensor networks rely heavily on FOLs for signal transmission. The reason behind this is that an FOL has the unique features of reduced dimensions and weight, wide bandwidth and immunity to electromagnetic interference. The information signals in an FOL are usually transmitted using intensity modulation, which allows direct detection at the receiver. Various intensity modulation schemes such as double sideband modulation, single sideband (SSB) modulation [2]–[8] and double sideband suppressed carrier modulation [9], [10] have been developed. While double sideband modulation can simply be implemented by applying the RF information signal to a Mach-Zehnder modulator (MZM) biased at the quadrature point, it suffers from the fibre dispersion problem causing output RF power degradation depending on the RF signal frequency and the length of the FOL. The fibre dispersion problem severely limits the RF signal bandwidth and the transmission distance.

Transmitting the optical carrier and only one sideband can overcome the fibre dispersion problem in a long-reach FOL. Optical SSB modulation is also required in various applications such as microwave photonic signal processing [11]–[13], optical coherence tomography [14], optical frequency shifter [15] and optical vector network analyser [16]. It can be realised by filtering out one sideband of a double sideband RF modulated optical signal. Different filtering techniques have been proposed, which include using a fibre Bragg grating [3], stimulated Brillouin scattering [4] and a tunable optical filter [5], [6]. Using the filtering technique for realising SSB modulation requires critical control on the wavelengths of the laser source and the optical filter to obtain a stable performance. The optical filter also needs to have a sharp edge roll off response to largely suppress the unwanted sideband close to the carrier frequency without altering the carrier and the wanted sideband. Another technique to realise SSB modulation is to apply two 90° phase difference RF signals to a quadrature-biased dual-drive MZM (DDMZM) [2] or a dual-parallel MZM [7]. This technique is widely accepted as it is independent to the optical carrier frequency. Note that since an MZM is a nonlinear device, it also generates higher order sidebands. It was pointed out in [8] that the presence of the second order sidebands results in some frequency dependent penalty in a long-reach radio-over-fibre system and causes measurement error in an optical vector network analyser. As such, a technique based on applying two 120° phase difference RF signals into a DDMZM has been proposed to suppress the second order sideband adjacent to the wanted first order sideband. However, the other second order sideband, which is adjacent to the suppressed first order sideband, remains unchanged. It beats with the optical carrier at the photodetector and generates the second order harmonic component at the FOL output. It should be pointed out that the second order harmonic component also presented in an FOL consisting of the conventional SSB modulator formed by a DDMZM and a 90° hybrid coupler. This is due to fibre dispersion that introduces different phase shifts to the $-$2nd and $+$2nd order sidebands.

In this paper, we propose for the first time a structure for realising SSB modulation without both the $-$2nd and $+$2nd order sidebands. The idea is based on using the second order sidebands generated by a maximum-biased DDMZM to cancel the second order sidebands generated by the conventional SSB modulator. This technique can realise broadband SSB modulation using only standard off-the-shelf components. It is independent to the optical carrier frequency. Experimental results are presented that demonstrate a SSB RF modulated optical signal with large suppression in the two second order sidebands, which leads to large reduction in the second order harmonic component compared to using the conventional SSB modulator in a long-reach FOL. Results also demonstrate the new optical SSB modulator exhibits carrier-frequency independent performance.

2. Operation Principle

Fig. 1 depicts the structure of the new optical SSB modulator. The main component is a dual-parallel DDMZM (DP-DDMZM), which consists of two DDMZMs (DDMZM-1 and DDMZM-2) with an optical phase shifter at one of the modulator outputs. DDMZM-1 is biased at the quadrature point and is driven by two 90° phase difference RF signals from a 90° hybrid coupler. It acts as a conventional SSB modulator with the $+$1st order sideband being suppressed as shown in Fig. 1. DDMZM-2 is biased at the maximum transmission point and is driven by two 180° phase difference RF signals from a 180° hybrid coupler. Therefore, the output of DDMZM-2 behaves like a single-drive maximum-biased MZM, which has an optical carrier and two second order sidebands as shown in the figure. Note that an attenuator is connected to the input of the 180° hybrid coupler. It is used to control the RF signal power into DDMZM-2 so that the amplitude of the $\pm$2nd order sidebands from DDMZM-2 is the same as that from DDMZM-1. An optical phase shifter connected to the output of DDMZM-2 changes the phase of the $\pm$2nd order sidebands from DDMZM-2 to ensure that the $\pm$2nd order sidebands in the top and bottom path of the DP-DDMZM are out of phase. The output of the phase shifter is combined coherently with DDMZM-1 output. Since the $\pm$2nd order sidebands in the top and bottom path have the same amplitude but opposite phase, they are cancelled at the DP-DDMZM output. On the other hand, the optical carriers in the top and

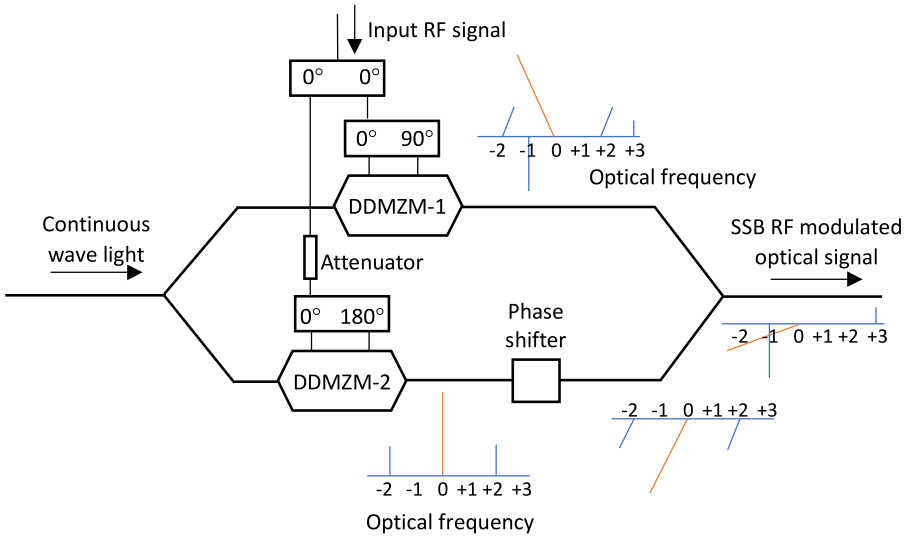

Fig. 1. New structure for optical single sideband modulation without the second order sidebands.

bottom path have a 90° phase difference rather than a 180° phase difference in the ±2nd order sidebands. Hence, they are combined and remain at the DP-DDMZM output.

The two DDMZMs and the optical phase shifter inside the DP-DDMZM are integrated on the same substrate and hence matching the two optical path lengths is not required. DP-DDMZMs are commercially available and can be made to have a very wide bandwidth. The power divider and hybrid couplers used in the DP-DDMZM based SSB modulator are standard commercial products, which are supplied by many microwave component manufacturers, and have a wide bandwidth. For example, Marki Microwave supplies a 4–40 GHz bandwidth 90° hybrid coupler with a cost of <$2000 USD [17]. On the other hand, the SSB modulation technique for suppressing only one of the second order sidebands requires a 120° hybrid coupler [8], which is not a standard product provided by microwave component manufacturers. Unlike the filter technique, the performance of the DP-DDMZM based SSB modulator is independent to the laser source wavelength and can be operated from few GHz microwave frequencies to tens of GHz millimeter wave frequencies limited by the hybrid coupler bandwidth.

3. Analysis and Simulation Results

Referring to Fig. 1, a continuous wave light with an angular frequency ω_c is launched into the DP-DDMZM, which is driven by an RF signal with an angular frequency ω_m. The electric field at the output of DDMZM-1 biased at the quadrature point is given by

$$E_{out1} = \left(\frac{E_{\text{in}}}{2}\right) t_{ff} \left[J_0(a)\cos\left(\omega_c t + \frac{\pi}{4}\right) - \sqrt{2}J_1(a)\cos(\omega_c - \omega_m)t + J_2(a)\cos\left((\omega_c - 2\omega_m)t - \frac{\pi}{4}\right) + J_2(a)\cos\left((\omega_c + 2\omega_m)t - \frac{\pi}{4}\right) + J_3(a)\cos(\omega_c + 3\omega_m)t\right] \quad (1)$$

where E_{in} is the amplitude of the electric field into the DP-DDMZM, t_{ff} is the insertion loss of the DDMZM and is assumed to be the same for both DDMZMs inside the DP-DDMZM, $J_m(x)$ is the Bessel function of mth order of first kind, $a = \pi V_{RF}/V_\pi$ is the modulation index, V_{RF} is the RF signal amplitude into DDMZM-1, V_π is the switching voltage of the DDMZM and is assumed to be the same for both DDMZM-1 and DDMZM-2. Note that the 4th and the higher order sidebands

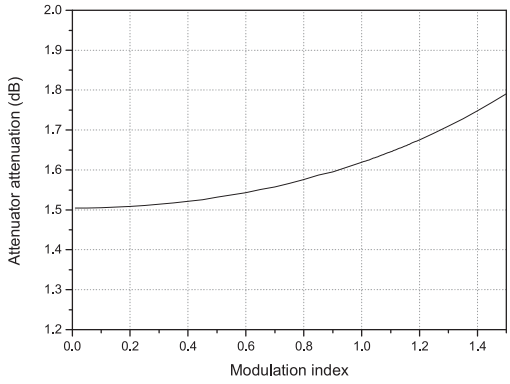

Fig. 2. Amount of attenuation required to cancel the second order sidebands at the output of the DP-DDMZM for different DDMZM-1 modulation indexes.

are neglected in the analysis as they are very small compared to the ±1st, ±2nd and ±3rd order sidebands. Equation (1) shows DDMZM-1 acts as a SSB modulator with the +1st order sideband at the frequency of $\omega_c + \omega_m$ being suppressed. It also shows the two ±2nd order sidebands from DDMZM-1 have the same phase of $-\pi/4$. The electric field at the output of DDMZM-2 biased at the maximum transmission point is given by

$$E_{out2} = \left(\frac{E_{\text{in}}}{\sqrt{2}}\right) t_{ff} \left[J_0(\alpha a)\cos(\omega_c t) + J_2(\alpha a)\cos(\omega_c + 2\omega_m)t + J_2(\alpha a)\cos(\omega_c - 2\omega_m)t\right] \tag{2}$$

where α is the amount of RF signal attenuation introduced by the attenuator at the 180° hybrid coupler input. It can be seen from (2) that the two ±2nd order sidebands from DDMZM-2 have the same phase and their phase difference is -π/4 compared to that from DDMZM-1. Therefore, the optical phase shifter after DDMZM-2 is designed to introduce 3π/4 phase shift to DDMZM-2 output to ensure the ±2nd order sidebands in the top and bottom path of the DP-DDMZM are out of phase. Hence the electric field at the output of the optical phase shifter is given by

$$E_{out2} = \left(\frac{E_{in}}{\sqrt{2}}\right) t_{ff} \left[J_0(\alpha a)\cos\left(\omega_c t + \frac{3\pi}{4}\right) + J_2(\alpha a)\cos\left((\omega_c + 2\omega_m)t + \frac{3\pi}{4}\right) + J_2(\alpha a)\cos\left((\omega_c - 2\omega_m)t + \frac{3\pi}{4}\right)\right] \tag{3}$$

The DP-DDMZM output electric field can be obtained by combining (1) and (3). It can be written as

$$E_{out} = \frac{E_{\text{in}} t_{ff}}{\sqrt{2}} \left[\sqrt{\left(\frac{J_0(a)}{2}\right)^2 + \left(\frac{J_0(\alpha a)}{\sqrt{2}}\right)^2}\cos\left(\omega_c t + \frac{\pi}{4} + \tan^{-1}\left(\frac{\sqrt{2}J_0(\alpha a)}{J_0(a)}\right)\right) - \sqrt{2}\left(\frac{J_1(a)}{2}\right)\cos(\omega_c - \omega_m)t + \left(\frac{J_2(a)}{2} - \frac{J_2(\alpha a)}{\sqrt{2}}\right)\cos\left((\omega_c - 2\omega_m)t - \frac{\pi}{4}\right) + \left(\frac{J_2(a)}{2} - \frac{J_2(\alpha a)}{\sqrt{2}}\right)\cos\left((\omega_c + 2\omega_m)t - \frac{\pi}{4}\right) + \frac{J_3(a)}{2}\cos(\omega_c + 3\omega_m)t\right] \tag{4}$$

Equation (4) shows both the −2nd and +2nd order sidebands have the same amplitude. They can be cancelled by designing the attenuator attenuation α. Fig. 2 shows the amount of attenuation required for the RF signal into DDMZM-2, to cancel the ±2nd order sidebands at the DP-DDMZM output for different modulation indexes.

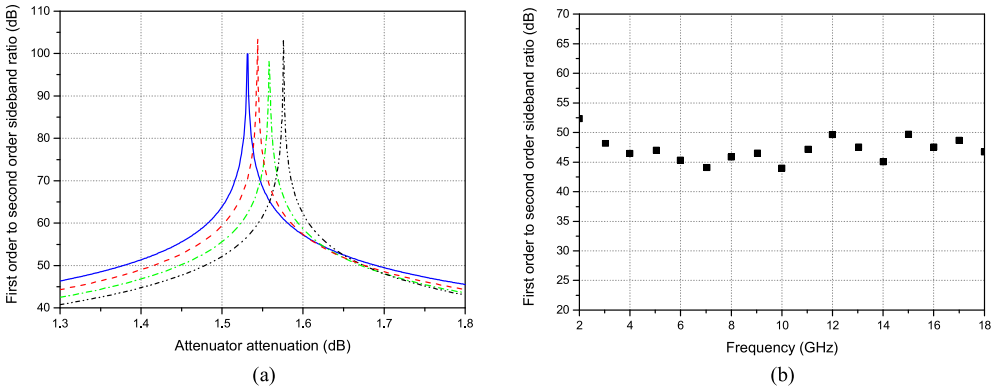

Fig. 3. Power ratio of the −1st and ±2nd order sideband generated by the DP-DDMZM based SSB modulator for (a) different attenuator attenuation and (b) different RF signal frequency. The DDMZM-1 modulation index is 0.5 (blue solid), 0.6 (red dash), 0.7 (green dot dash) and 0.8 (black dot dot dash).

It can be seen from the figure that the required amount of attenuation for cancelling the ±2nd order sidebands remains almost the same for different modulation indexes if the input RF signal is a small signal. There is <0.2 dB change in the attenuator attenuation needed to fully cancel the ±2nd order sidebands for a large change in the modulation index from 0.01 to 1.2. The output optical power is the output electric field magnitude squared, that is

$$P = |E_{out}|^2 \tag{5}$$

The power ratio of the −1st and ±2nd order sideband at the output of the DP-DDMZM, which can be obtained from (5), was investigated for different modulation indexes and different attenuator attenuation. Fig. 3(a) shows a high −1st and ±2nd order sideband power ratio of >60 dB can be obtained by using a 1.56 dB attenuator for a DDMZM-1 modulation index between 0.5 and 0.8. This shows large suppression in the ±2nd order sidebands can be obtained using a fixed attenuator attenuation for a range of modulation indexes.

In practice, couplers have amplitude and phase imbalance, which affects the amount of the ±2nd order sideband suppression. Simulation was conducted using a photonic simulation software to investigate the effect of the 90° hybrid coupler amplitude and phase imbalance on the DP-DDMZM based SSB modulator ±2nd order sideband suppression. The coupler amplitude and phase imbalance used in the simulation were obtained by measuring the amplitude and phase response of a 2–18 GHz bandwidth 90° hybrid coupler using a vector network analyser. Fig. 3(b) shows the simulated DP-DDMZM based SSB modulator first to second order sideband power ratio at different RF signal frequencies for 1.56 dB attenuator attenuation. It can be seen that more than 44 dB first to second order sideband power ratio can be obtained over the 2–18 GHz frequency range. Note that the measured amplitude and phase response of the 2–18 GHz bandwidth 90° hybrid coupler show this coupler has an amplitude imbalance of <±0.6 dB and a phase imbalance of <±3° over the 2–18 GHz frequency range. More than 15 dB ±2nd order sideband suppression within the 90° hybrid coupler operating bandwidth of 16 GHz can be obtained for this amplitude and phase imbalance. It was found from the simulation result that the 90° hybrid coupler amplitude and phase imbalance need to be within ±0.25 dB and ±1.5° in order to suppress the ±2nd order sidebands by more than 20 dB when comparing with the conventional DDMZM based SSB modulator. Slight adjustments on the attenuator attenuation and the modulator bias voltages can reduce the effect of the coupler amplitude and phase imbalance on the ±2nd order sideband suppression. Commercial wideband 4–40 GHz 90° hybrid couplers have typical amplitude and phase imbalance of ±0.4 dB and ±5° respectively [17]. This reduces the ±2nd order sideband suppression to 12 dB, which corresponds to a maximum of 24 dB suppression in the second order harmonic after photodetection.

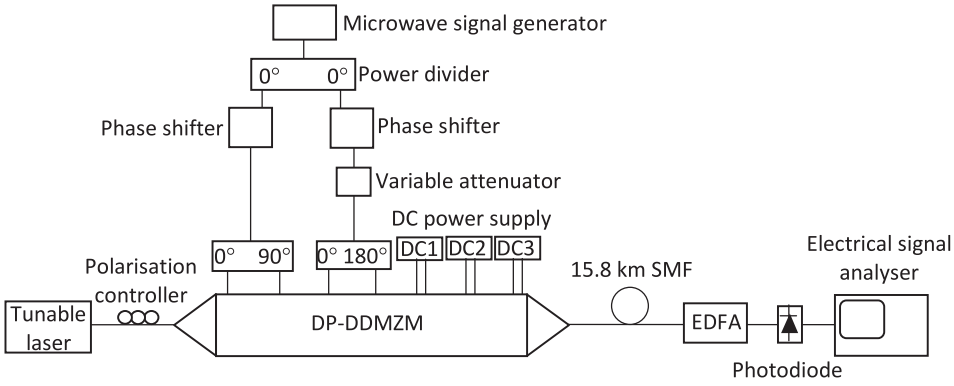

Fig. 4. Experimental setup of an FOL using a DP-DDMZM to generate a SSB RF modulated optical signal.

In a long-reach FOL, the SSB RF modulated optical signal from the DP-DDMZM passes through a length of fibre and is detected by a photodiode at the receiver. The output photocurrent consists of the original RF information signal and the harmonic components. The photocurrent at the second order harmonic angular frequency $2\omega_m$ is given by

$$I_{2\omega m} = \frac{\Re P_{\text{in}} {t_{ff}}^2}{2}\left(\frac{J_2(a)}{2} - \frac{J_2(\alpha a)}{\sqrt{2}}\right)\sqrt{\left(\frac{J_0(a)}{2}\right)^2 + \left(\frac{J_0(\alpha a)}{\sqrt{2}}\right)^2} \cdot \sqrt{(\cos(\theta-\phi_1) - \cos(\theta-\phi_2))^2 + (\sin(\theta-\phi_1) + \sin(\theta-\phi_2))^2} \quad (6)$$

where

$$\theta = \tan^{-1}\left(\frac{J_0(\alpha a)\sqrt{2}}{J_0(a)\,2}\right) \quad (7)$$

ϕ_1 and ϕ_2 in (6) are the optical phase difference between the optical carrier and the $-$2nd and $+$2nd order sideband introduced by fibre dispersion respectively, P_{in} is the optical power into the DP-DDMZM and $\Re$ is the photodiode responsivity. Equation (6) shows that, regardless the amount of optical phase shift added to the second order sidebands, the second order harmonic component of the DP-DDMZM based FOL can be eliminated by introducing around 1.55 dB attenuation to the RF signal into DDMZM-2.

4. Experimental Results

An FOL consisting of a DP-DDMZM was set up as shown in Fig. 4 to verify the new SSB modulation technique does not generate $\pm$2nd order sidebands and has no second order harmonic component at the FOL output. The optical source was a wavelength tunable laser operated at 1550 nm. The continuous wave light from the optical source passed through a polarisation controller, which was used to align the light to the slow axis of the fibre before launching into a DP-DDMZM (Sumitomo T.SBXH1.5-20PD-ADC). This modulator had two pairs of RF ports connected to the two DDMZMs. A 13 GHz RF signal generated by a microwave signal generator (Analog Devices HMC-T2220) was split equally into two via a power divider. The outputs of the power divider were connected to two electrical phase shifters, which were used to match the electrical path lengths between the power divider and the two DDMZMs. An electrical variable attenuator was connected to one of the phase shifter outputs to control the $\pm$2nd order sideband amplitudes generated by DDMZM-2. The RF signals were split via a 90° hybrid coupler (Krytar 1830) and a 180° hybrid coupler (Gwave GHC-180-010180), which were then applied to DDMZM-1 and DDMZM-2 respectively. The two DDMZMs were biased at the quadrature point and the maximum transmission point as

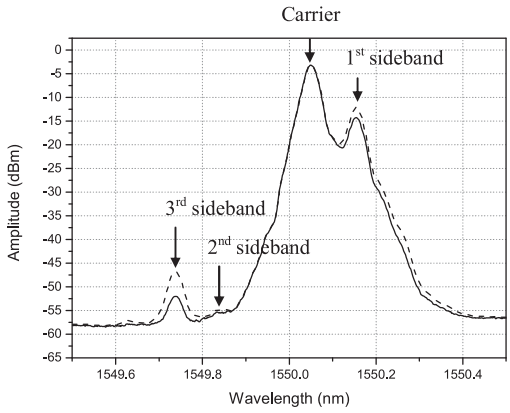

Fig. 5. Measured output spectrum of the DP-DDMZM driven by a 13 GHz RF signal with a DDMZM-1 modulation index of 0.52 (solid) and 0.68 (dashed).

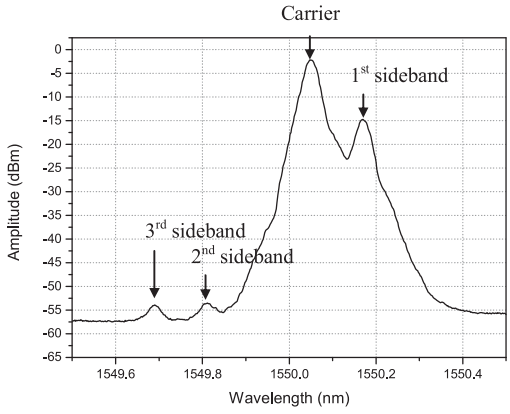

Fig. 6. Measured output spectrum of the DP-DDMZM driven by a 15 GHz RF signal with a DDMZM-1 modulation index of 0.52.

was discussed in Section 2. The optical phase difference between the two DDMZM outputs was controlled via a DC voltage into the main MZM of the DP-DDMZM. The output of the DP-DDMZM was observed on an optical spectrum analyser.

The electrical variable attenuator was adjusted to suppress the $\pm$2nd order sidebands at the DP-DDMZM output. It was found that the attenuator attenuation required to largely suppress the $\pm$2nd order sidebands was 1.6 dB, which agrees with theory. Fig. 5 shows the DP-DDMZM output spectrums for different modulation indexes. It can be seen that the $\pm$2nd order sidebands are $>$42 dB below the $-$1st order sideband for both DDMZM-1 modulation index of 0.52 and 0.68. Note that the horizontal axis of the optical spectrum shown in Fig. 5 is displayed in wavelength. Hence the sideband on the right of the optical carrier has a lower optical frequency than the left sideband. Therefore, the right first order sideband in Fig. 5 is actually the $-$1st order sideband. Large suppression in the $\pm$2nd order sidebands was also demonstrated for different input RF signal frequencies. For example, Fig. 6 shows the $\pm$2nd order sidebands are 38.8 dB below the $-$1st order sideband when the input RF signal frequency was changed from 13 GHz to 15 GHz. Note that the slight increase in the $\pm$2nd order sideband amplitude for a 15 GHz input RF signal is due to the electrical components and the modulator used in the experiment have a slight frequency dependent characteristic. The wavelength of the optical source was changed from 1550 nm to 1540 nm and 1560 nm to demonstrate the performance of the DP-DDMZM based SSB modulator is insensitive to the optical source wavelength. The DP-DDMZM output spectrums in Fig. 7, which were obtained

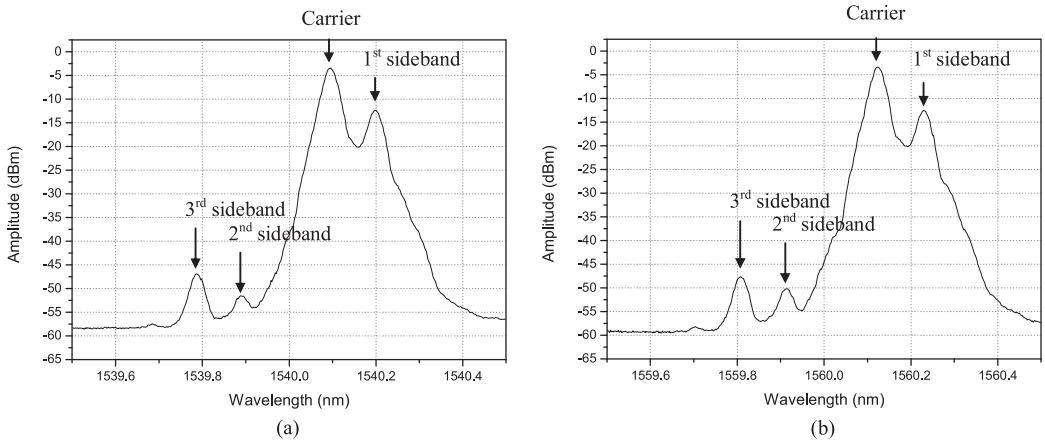

Fig. 7. Measured output spectrum of the DP-DDMZM for a laser source wavelength of (a) 1540 nm and (b) 1560 nm.

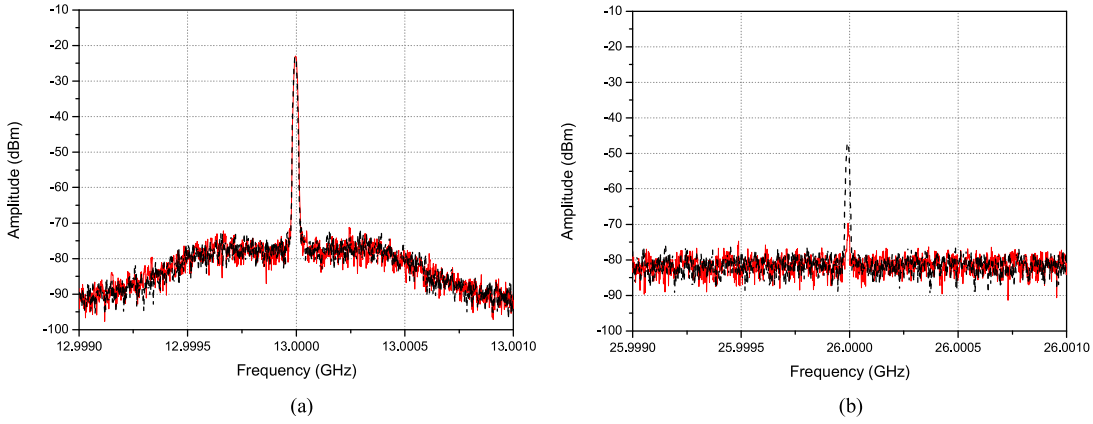

Fig. 8. Measured output spectrum of a fibre optic link consisting of a DP-DDMZM (red solid line) and a single DDMZM (black dashed line) at (a) the fundamental RF signal frequency and (b) the second order harmonic RF signal frequency.

without readjusting the attenuator attenuation after changing the optical source wavelength, show the $\pm$2nd order sidebands remain below the $+$3rd order sideband.

The second order harmonic nonlinearity of a FOL consisting of a DP-DDMZM was investigated. This was done by connecting the DP-DDMZM output to a 15.8 km long standard single mode fibre (SMF). This was followed by an erbium doped fibre amplifier (EDFA) and a 22 GHz bandwidth photodiode (Discovery Semiconductors DSC30S) as shown in Fig. 4. The DP-DDMZM was driven by a 13 GHz RF signal and had an output optical spectrum as shown by the solid line in Fig. 5. The average optical power into the photodiode was 3.6 dBm. The red solid line in Fig. 8(a) and (b) show the FOL output spectrum measured on an electrical signal analyser at 13 GHz and 26 GHz respectively. Due to the large suppression in the $\pm$2nd order sidebands, the second order harmonic component at the DP-DDMZM based FOL output is more than 46 dB below the fundamental component at 13 GHz.

Finally, a FOL formed by a single DDMZM (Fujitsu FTM7937EZ200) with a 90° hybrid coupler connected to the modulator RF input ports was also set up for comparison. The RF signal power into the single DDMZM was adjusted to ensure the amplitude ratio of the optical carrier to the wanted first order sideband was the same as that for the DP-DDMZM output shown in Fig. 5. The output spectrums of the single DDMZM driven by a 13 GHz RF signal with different modulation indexes

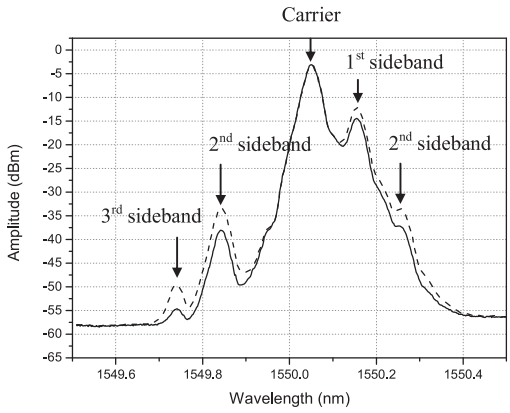

Fig. 9. Measured output spectrum of the single DDMZM driven by a 13 GHz RF signal with different RF signal powers into the modulator so that the carrier to −1st order sideband power ratio is the same as that for the DP-DDMZM shown in Fig. 5.

are shown in Fig. 9. It shows as expected the −2nd and +2nd order sidebands are presented at the single DDMZM output. The experimental results demonstrate using a DP-DDMZM can realise SSB modulation with >20 dB ±2nd order sideband suppression compared to using a single DDMZM. The output of the FOL consisting of a single DDMZM and a 15.8 km long standard SMF was measured on an electrical signal analyser. The gain of the EDFA in an FOL was adjusted so that the optical power into the photodiode was 3.6 dBm, which was the same as that for the DP-DDMZM based FOL. The dashed line in Fig. 8(a) and (b) show the single DDMZM based FOL output spectrum at 13 GHz and 26 GHz respectively. It can be seen from Fig. 8(a) that the output fundamental RF signal amplitudes are the same for both FOLs. However, the second order harmonic component generated by the DP-DDMZM based FOL is 22.6 dB below the single DDMZM based FOL.

5. Conclusion

A new structure for realising SSB modulation without generating both −2nd and +2nd order sidebands has been presented. It is based on using the two ±2nd order sidebands generated by a maximum-biased DDMZM to cancel with that generated by the conventional SSB modulator formed by a single DDMZM with a 90° hybrid coupler at the modulator RF input ports. Cancelling the ±2nd order sidebands in a SSB modulator not only has the advantage of reducing the measurement error in an optical vector network analyser but also eliminating the second order harmonic component in a long-reach radio-over-fibre system. Unlike the technique that suppresses only one second order sideband, here both −2nd and +2nd order sidebands are suppressed and only standard off-the-shelf components are required. The analysis and design procedure for the new SSB modulator has been described. The new SSB modulator has been experimentally verified, and results have been presented for this SSB modulator that demonstrate both the ±2nd order sidebands are largely suppressed to >42 dB below the −1st order sideband and the second order harmonic component is >46 dB below the fundamental RF signal at the output of an FOL consisting of a DP-DDMZM and a 15.8 km long standard SMF.

References

[1] D. Novak *et al.*, "Radio-over-fiber technologies for emerging wireless systems," *IEEE J. Quantum Electron.*, vol. 52, no. 1, pp. 1–11, Jan. 2016.
[2] G. H. Smith, D. Novak, and Z. Ahmed, "Overcoming chromatic-dispersion effects in fiber-wireless systems incorporating external modulators," *IEEE Trans. Microw. Theory Techn.*, vol. 45, no. 8, pp. 1410–1415, Aug. 1997.
[3] J. Park, W. V. Sorin, and H. Y. Lau, "Elimination of the fibre chromatic dispersion penalty on 1550 nm millimeter-wave optical transmission," *Electron. Lett.*, vol. 33, no. 6, pp. 512–513, Mar. 1997.

[4] Y. C. Shen, X. Zhang, and K. Chen, "Optical single sideband modulation of 11-GHz RoF system using stimulated Brillouin scattering," *IEEE Photon. Technol. Lett.*, vol. 17, no. 6, pp. 1277–1279, Jun. 2005.
[5] X. Wang, J. Zhang, E. H. W. Chan, X. Feng, and B. Guan, "Ultra-wide bandwidth photonic microwave phase shifter with amplitude control function," *Opt. Exp.*, vol. 25, no. 3, pp. 2883–2894, 2017.
[6] Z. Tang, S. Pan, and J. Yao, "A high resolution optical vector network analyzer based on a wideband and wavelength tunable optical single-sideband modulator," *Opt. Exp.*, vol. 20, no. 6, pp. 6555–6560, 2012.
[7] B. Hraimel *et al.*, "Optical single-sideband modulation with tunable optical carrier to sideband ratio in radio over fiber systems," *J. Lightw. Technol.*, vol. 29, no. 5, pp. 775–781, Mar. 2011.
[8] M. Xue, S. Pan, and Y. Zhao, "Optical single-sideband modulation based on a dual-drive MZM and a 120° hybrid coupler," *J. Lightw. Technol.*, vol. 32, no. 19, pp. 3317–3323, Oct. 2014.
[9] R. D. Esman and K. J. Williams, "Wideband efficiency improvement of fiber optic systems by carrier subtraction," *IEEE Photon. Technol. Lett.*, vol. 7, no. 2, pp. 218–220, Feb. 1995.
[10] K. J. Williams and R. D. Esman, "Stimulated Brillouin scattering for improvement of microwave fibre-optic link efficiency," *Electron. Lett.*, vol. 30, no. 23, pp. 1965–1966, Nov. 1994.
[11] R. A. Minasian, E. H. W. Chan, and X. Yi, "Microwave photonic signal processing," *Opt. Exp.*, vol. 21, no. 19, pp. 22918–22936, 2013.
[12] J. Yang, E. H. W. Chan, X. Wang, X. Feng, and B. Guan, "Broadband photonic microwave phase shifter based on controlling two RF modulation sidebands via a Fourier-domain optical processor," *Opt. Exp.*, vol. 23, no. 9, pp. 12100–12110, 2015.
[13] M. Sagues, R. G. Olcina, A. Loayssa, S. Sales, and J. Capmany, "Multi-tap complex-coefficient incoherent microwave photonic filters based on optical single-sideband modulation and narrow band optical filtering," *Opt. Exp.*, vol. 16, no. 1, pp. 295–303, 2008.
[14] Z. He, Q. N. Ho, W. Zou, K. Kajiwara, H. Takahashi, and K. Hotate, "Optical coherence tomography based on optical frequency comb generator with single-sideband modulator," in *Proc. 15th OptoElectron. Commun. Conf.*, 2010, pp. 802–803.
[15] H. Chen and E. H. W. Chan, "Optical frequency shifter employing Brillouin assisted filtering technique," *IEEE Photon. J.*, vol. 9, no. 2, Apr. 2017, Art. no. 7102111.
[16] R. Hernández, A. Loayssa, and D. Benito, "Optical vector network analysis based on single-sideband modulation," in *Proc. 16th Annu. Meeting IEEE Lasers Electro-Opt. Soc.*, 2003, vol. 2, pp. 909–910.
[17] Marki Microwave 90° modules, 2018. [Online]. Available: http://www.markimicrowave.com/hybrids/hybrids-products.aspx#90degree-Modules